Detection of Pulmonary Nodules Based on a Template-Matching Technique

Sérgio Eduardo de Almeida e Mota – ee98171@fe.up.pt

Abstract-**The purpose of this study is to develop a simple technique for computer-aided diagnosis (CAD) system to detect lung nodules in chest radiographic images. A conventional template matching was employed to detect the nodules, and after initial detection, we extracted 7 feature values and used them to eliminate false-positives findings. Despite the expected, the project never had the contributions of a professional physician, so the results are deprived of any medical verification. Given this, we aimed at the detection of every circular abnormalities (that most likely will correspond to pulmonary nodules).**

I-INTRODUCTION

Lung cancer is one of the most serious cancers in the world. Of all the types of cancer, lung cancer is the most common cause of death and accounts for about 28% of all cancer deaths. At the same time, it appears that the rate has been steadily increasing. Not smoking is considered the most effective way to reduce the incidence of lung cancer in most countries, while detection of suspicious lesions in the early stages of cancer can be considered the most effective way to improve survival.

Chest X-ray image has been used for detecting lung cancer for a long time. The early detection and diagnosis of pulmonary nodules in chest X-ray image are among the most challenging clinical tasks performed by radiologists as it is well established that they may miss up to 30% of pulmonary nodules in an exam. Interpreting a chest radiograph is extremely challenging. Superimposed anatomical structures make the image complicated. Even experienced radiologists have trouble distinguishing infiltrates from the normal pattern of branching blood vessels in the lung fields, or detecting subtle nodules that indicate lung cancer. When radiologists rate the severity of abnormal findings, large interobserver and even intraobserver differences occur. In addition, since the majority of screening cases are normal, diagnostic reading errors may be hard to avoid.

Computer-aided diagnosis (CAD) has been proven to be a very effective approach as assistant to radiologists for improving diagnostic accuracy by providing a "second opinion" and therefore may be used in the first stage of examination in the near future. With the current advent of digital radiography systems, we firmly believe that development and application of artificial intelligence techniques for the automated screening of nodules will have a great impact on early detection of lung cancer.

Numerous systems were reported for detecting lung nodules on chest X-ray images. However, the strong concern of almost all of them is that the false positives per image are too large. How to reduce the number of false positives while maintaining a high true positive detection rate is the most important work in designing a chest CAD system. Most of the proposed computer-aided diagnosis systems (CAD systems) adopt a two-stage approach.
Typically, the first stage uses some kind of initial linear processing, which has high sensitivity and low specificity, to detect a set of potential nodules. The second stage consists in classifying these suspicious regions using a pattern recognition approach, which is a combination of a feature extraction process and a classification process using neural network classifier or statistical classifier. The performance of the classifier depends directly on the ability of characterization of candidate regions by the adopted features.

In this paper, we investigate a simple scheme to automatically detect pulmonary nodules in chest X-Ray images. The scheme uses a simple classical template-matching method in which a nodular model with Gaussian distribution is used as a reference pattern to select the candidate regions that may or may not contain a solitary pulmonar nodule.
To classify these areas several measures were conducted over a thresholded candidate using classical features like the ones cited in [1] and [2].

II. MATERIALS AND BACKGROUNDS

DATA SET

Thirty-nine posteroanterior chest radiographs were used in this study. All radiographs were obtained from the INEB research team database at FEUP. The digital chest images had 10-bit gray-scale resolution. For better viewing and faster processing, each input image was first subsampled to 8-bit gray-scale resolution with one-fourth of the original size. Although the data set is not large, the cases are a good representation of different kinds of chest images (ie, images were normal or abnormal, showed regular or irregular lung shapes, and were obtained from both sexes).

CONSIDERATIONS

In spite of the expected, during this study it was not possible to rely on the opinion of a specialist physician that would have done a pre-detection of solitary nodules based on his professional experience; that "visual processing" should be an obligatory task to the correct orientation of the workflow in the sense that one then would have the basis for posterior correlation with the study results. Therefore, it was determined since the beginning that the classification of the suspicious areas would be done regarding the detection of ANY circular structures, which in reality could be nodules, blood vessels, bones or bronquial complexes (e.g. Fig. 1,2,3,4). Since the objective of this work was the creation of a CAD system that could provide a second opinion to a radiologist visually inspecting x-ray's, the task of separating the carcinomas from other structures was left for him to perform, given that a good help has already been given by automatically selecting non-spiculated mainly circular regions.

III. METHODS

To detect pulmonary nodules, we've employed a template-matching approach based on simple models that simulate real nodule. Lung nodules were classified regardless of medical classification.

Nodules within the lung area tend to have spherical shapes, but some of them may be semicircular: according to the torax position during the patient exposure's to the X-Rays, or that are simply localized on the lung wall; therefore those will not be part of this work scope of detection even tough they are also important to detect in a early phase of development.

The procedural flowchart of this project is shown in Fig. 5.

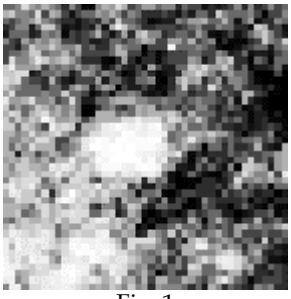

Fig. 1

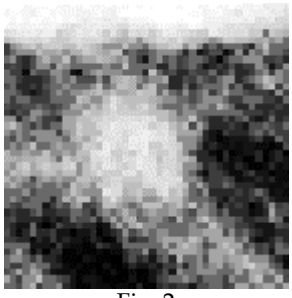

Fig. 2

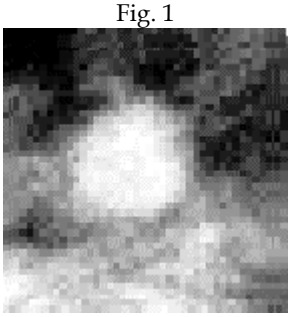

Fig. 3

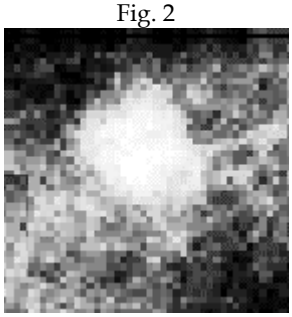

Fig. 4

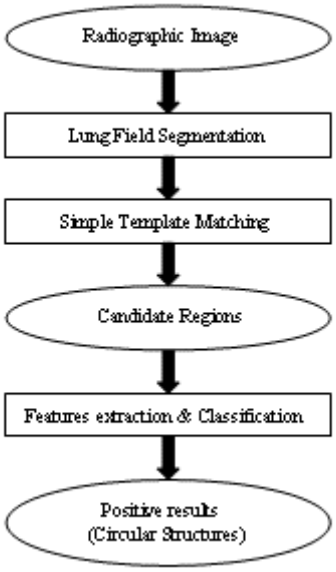

Fig. 5

A-LUNG FIELDS SEGMENTATION

Automatic segmentation of the lung fields is virtually mandatory before computer analysis of chest radiographs can take place. Several studies deal with this problem exclusively. In the research herein presented we focused in obtaining just a simple rectangular framing able to delimitate each left and right lung field independently. The early detection of right and left regions of interest (ROIs) allows for a decrease in computation time of subsequent project

steps and follows the basic principle that the areas outside the lungs have no interest whatsoever to the objective of this project, and so, therefore, they should be, if possible, ignored. The methods used in this step were partially based on the study developed in Monteiro,Mendonça & Campilho [3] with some minor changes.

Each rectangular area is delimited by four lines, beeing one of them common to the two lung field ROIs. This line is expected to be aligned along the direction of the mediastinum, and, therefore, dividing the image into two parts, corresponding to each lung area. The position of this separation line is obtained from the location of the absolute maximum of the intensity projection of the complete image. This choice is justified because the area between the two lung fields is usually brighter, as a consequence of the greater absorption capability of the vertebral column and abdomen. (Fig. 6).

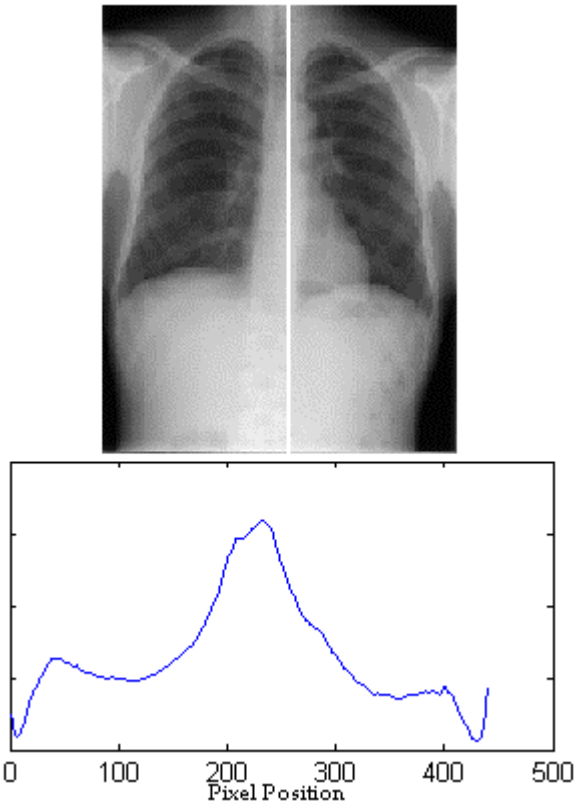

Fig. 6 (with central line superimposed) with profile of the image projection onto the horizontal axis

Then, separately for the left and right parts of the image the following steps are applied in an identical manner except for positional reflection imposed by simmetry.

The procedure used to delimitate each lung field is based on the analysis of the profiles that result from a sequence of vertical and horizontal intensity projections, where the area of projection is consecutively reduced while refining lung field limits.

Initial estimates for the top and bottom lines of the ROI are obtained from the projection of image intensities onto the vertical axis. The bottom line position is obtained from the profile maximum point. The initial location for the top line is the line corresponding to the first 10% of the total number of lines, as the initial lines of the used data set usually contain disturbing intensity values, not corresponding to the lung regions. With these two limits defined, the image area between them is projected onto the horizontal direction. The analysis of the projection profile allows the association of lung region with the minima in the profile medial region. The search for the absolute maximum to the left (right) indicates the position of the lateral limit of the right (left) lung field.

In order to refine the ROIs top and bottom limits, the vertical stripe defined by the central line and the left (right) line image columns is once again projected onto the vertical axis. The new value for the top lines is obtained from the position of the absolute maximum contained in the left (right) 3% - 30% region of that projection. The new position for each of the bottom lines cannot be obtained directly from the projection profile because the ideal position is usually located in the greatest climbing zone in the right half of the profiles. As this position normally coincides with the highest increase in the projection values, the maximal point in the projection profile derivative is assumed as a candidate for bottom line position. However, this new value is retained only if it's lower than the initial bottom lines estimates. (Fig. 7, 8)

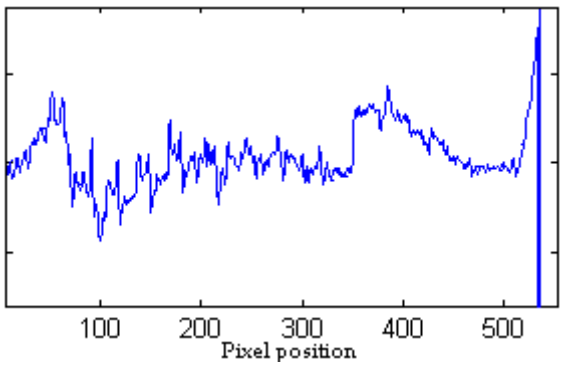

Fig. 7 – vertical projection of the stripe defined by the mediastinal line and the initial left line, used to calculate the new top line position

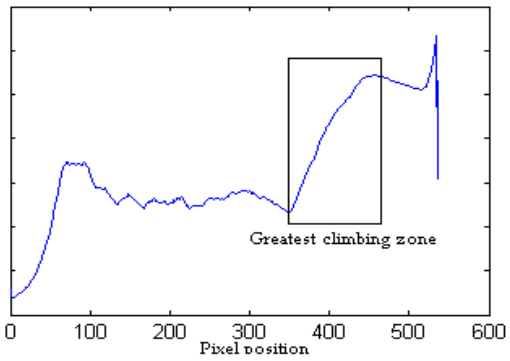

Fig. 8 – derivative of the profile in Fig. 7

Further refinements of the lateral lines is achieved when the areas between the top line and the bottom line limits are divided into four quadrants and the fourth one (the one that most likely will contain the costophrenical angle - Fig. 9), is once again projected onto the horizontal direction. The position of the maximum in this profile defines the final lateral limits. Even so, this method doesn't achieve perfection (at least in most of the available test set radiographies), and so, some further correction possibilities must be given to the physician in order to enable a precise user-corrected delimitation before the process can continue.

B-DETECTION SCHEME

To detect these pulmonary nodules/circular objects, we employed a template-matching approach based on a simple model that simulates real nodules as the reference images. Chest radiographs inherently display a wide dynamic range of X-ray intensities which permited us to observe the ocurrence of a Gaussian distribution around the center of each probable nodule; so, to verify this possibility, the full data set of reduced size radiographs was used to create a library of visually-chosen 59 structures who might or might not be nodules, but which for sure represented a circular object that should constitute an output of the template matching operation. Each entry of this new data set was a 9 x 9 pixel subimage (independently of the size and shape of the pictorized structure). This library was then used to calculate the intensity values average profile around horizontal and vertical directions perpendicular to each other and that crossed the center of the subimage (pixel (5,5)). These tend, as said, to follow a Gaussian distribution, as shown in Fig. 10 for the horizontal direction. Therefore, given the results, it was assumed that the proposed approximation was viable and the model was designed in the basis of the formulation refered by Lee & others [4]:

$$pv_{xy} = m \cdot e^{-(x^2+y^2)/n}$$

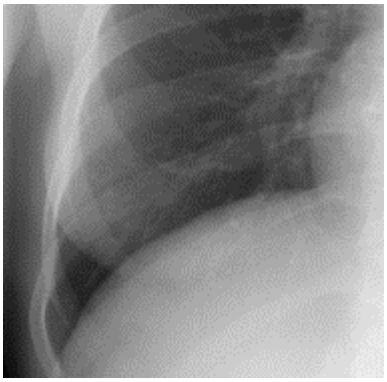
Fig. 9 – Costophrenical angle

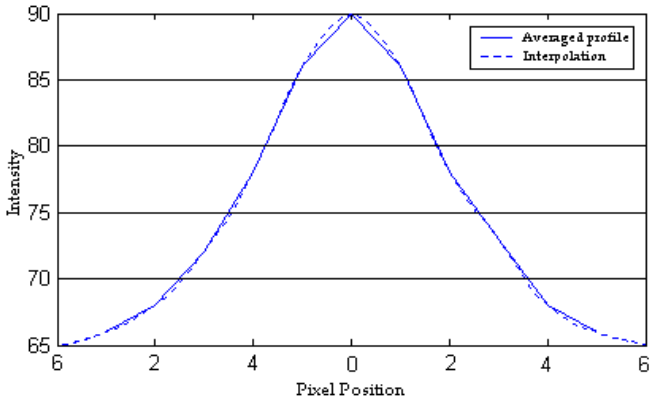

Fig. 10 – Average profile of intensity values for 59 nodules

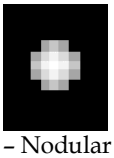
Fig. 11 – Nodular model

where pv_{xy} is the pixel intensity value of coordinate (x,y) , and m and n are parameters representing the maximum value and variance of the distribution, respectively. These parameters were decided experimentally during the test phase in a way to maximize the number of detected objects after the subsequent template-matching.

The circular structures visually chosen at the creation of the nodule library all had an average diameter of 7 pixel, and, since the subimages were all 9x9 pixel, our intention to solely work over nodules with less than 9 pixels in diameter is implicit. Ocurrences bigger than this ones were ignored in the construction of the model but nevertheless some of them may be detected since they can also have a Gaussian distribution around the middle point.

The final model can be seen on Fig.11.

A conventional template matching was employed to detect nodules. The "fitness" between the low resolution pulmonar image and the reference model may be described through the normalized cross-correlation coefficient, defined as:

$$\gamma(u,v)=\frac{\sum_{x,y}\left[f(x,y)-\overline{f_{u,v}}\right]\cdot\left[t(x-u,y-v)-\bar{t}\right]}{\sqrt{\sum_{x,y}\left[f(x,y)-\overline{f_{u,v}}\right]^2\cdot\sum_{x,y}\left[t(x-u,y-v)-\bar{t}\right]^2}}$$

in which *f(x,y)* is the pulmonary image and *t(x,y)* is the model image. The cross-correlation coefficient varies from -1 to 1 (by the Cauchy–Schwarz inequality), and does not depend on the intensity values but only on the shape of the pixel value distribution in both images *f* and *t*. As a result, an image result was obtained in which each pixel depicts the correlation coefficient between the template and the original picture at that point. If this value exceeds a given detection threshold then the region centered at the given point is taken as containing a structure similar to the modelized nodule, and so, it should constitute a suspicious region and consequently admitted to further processing steps for feature evaluation. A "suspicious zones" data set is therefore built and each entry is a 43x43 pixel subimage cointaining that area withdrawn from the high resolution version of the investigated X-ray image.

C-CLASSIFICATION SCHEME

Our detection scheme encountered numerous nodule candidates that are not clearly circular in shape, so, it became necessary to develop some method to eliminate them.The clinical user's "knowlegde of" and experience with the data in the context of this application would suggest features that should be evaluated to reliably automate this true/false result separation, but as we said, none was available for assistance, and therefore, our visually (and opinion-based) acessement doesn't guarantees that the classifier will perform as well on a new set of radiographies. An image feature is a distinguishible primitive characteristic or attribute that enables the identification of regions with common properties within an image or several images; in this case, it's the commonly obvious circularity inherent to any nodular structure that we wish to seek for.

For each calculation of the features' values a thresholded version of the suspicious area is constructed supposing that it posesses a (mean-filtered-length 5) histogram with an approximated bimodal shape. The threshold value is obtained as depicted in Fig. 12 - for each intensity level, it is the value corresponding to the biggest distance between it's frequency count and the line connecting the last maximum count and the last intensity that hasn't null count. Some further processing is applied over each binarized region in order to smooth it and eliminate smaller and non-centered portions that do not correspond to the potential nodule that must be on the middle of the subimage. For this, every connected component that touches the boundary of the image or has area smaller than a beforehanded found maximum is deleted. At this point the binarized region should contain only a centered component, so, some morphological transformations (a Dilation→Erosion→Dilation sequence) are applied in order to eliminate existent holes that could invalidate feature evaluations.

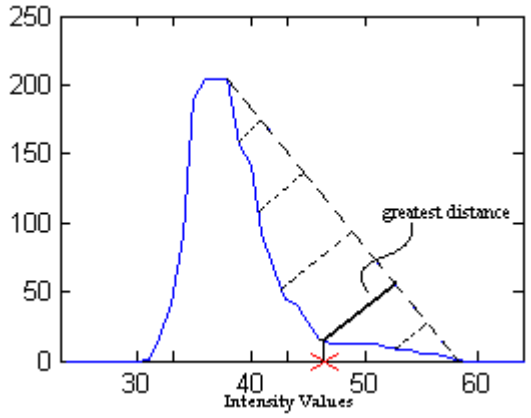

Fig. 12 – Method for obtaining treshold value applied over a mean-filtered histogram (filter length=5)

We employed several shape descriptors as our classification features:

1) Mean of the subimage containing the suspicious area: There were parts of bone and mediastinum which appeared to have a concentration distribution similar to the nodular model. Therefore, this feature is implemented to recognize these false positives.

2) Area, Circularity and Solidity of suspicious region: Considering that a nodule has a limited size and appears circular in a radiographic image, it is possible to recognize false positives by the shape and size of the candidates. Therefore, area, circularity and solidity were introduced as features to delimit FP's. Solidity was defined as the ratio of the area of an object to the area of a convex hull of the object (alternatively, as the density of the object).

Circularity was defined to be the ratio of the area of an object to the area of a circle with the same convex perimeter: ($=4x\pi x$Area/Convex Perimeter^2). All these features are calculated from the binarized candidate

region, and to be deemed a true positive their values must be in a range such that Area (pixels) ≥ t_1 (to prevent/despise errors on the tresholding), Circularity ≥ t_2 and Solidity ≥ t_3.

3) Centroid position and Elongation for the suspicious area: The centroid position is calculated to once again provide a means to despise bad thresholding results (generally the cases in which the suspicious area histogram isn't bimodal); only the centroids located in the inner 5x5 area of the 43x43 subimage are considered, beeing all the others automatically entitled false posiives. The Elongation enhances the TP classification by acceptting suspicious zones that the binarization distorted to near-elliptical shapes but that can altogether be true nodules. To be deemed a true positive it's value must be in a range such that Elongation ≤ t_4.

4) Radial distance standard deviation: The shape of a structure of interest can be determined by analysing its boundary, the variations and curvature of which constitute the information to be quantified. The radial distance d(n) is measured from the central point (centroid) in the object to each pixel x(n), y(n) on the perimeter (Fig.13). To achieve scale invariance, the normalised radial distance r(n) is obtained dividing d(n) by the maximal distance. To be deemed a true positive their values must be in a range such that Standard deviation ≤ t_5.

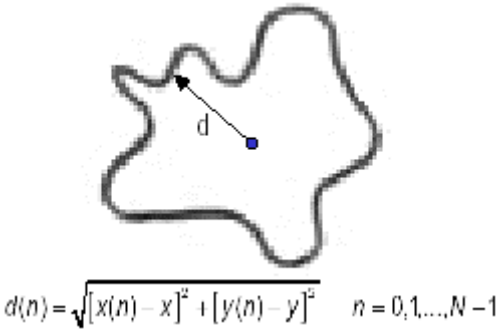

Fig. 13 – Definition of radial distance

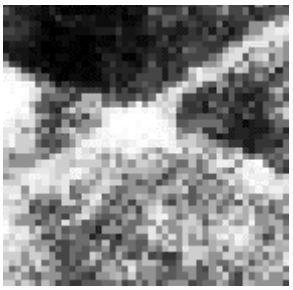

Fig. 14 – Rib crossing

IV. DETECTION PERFORMANCE

Our method was applied to 22 X-ray images of the original data set. Since we don't have the means to detect any true nodules, only the classification step as been evaluated: given all the detected structures found by template matching, the number of obvious visually-confirmed circular objects found ranged from 2 to 16/case, but a lot other true positives were found although they do not appear to have the required shape. At this cases it would be up to the physician to classify the results. These bodies may not be nodules but it was observed that generally they correspond to rib crossings (Fig. 14), intersecting blood vessels (Fig. 15) or small protrusions on a rib border (Fig.16). For the values t_1=20, t_2=0.723,t_3=0.81,t_4=1.71 and t_5=0.173 we found that the system detected 116 of 171 clearly circular shapes, although other 158 regions lacking this property were deemed as TP's.

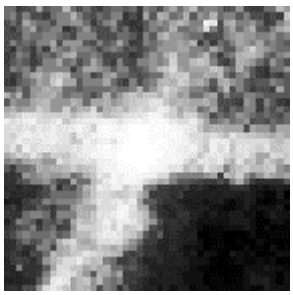

Fig. 15

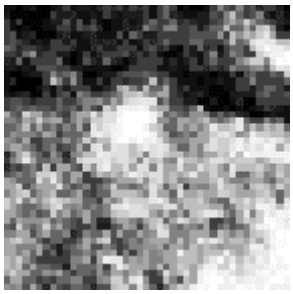

Fig. 16

V. DISCUSSION

The cases used in this study included many nodules/circular structures with diameters bigger than the 7 pixels wide of the used model, and, though some were correctly detected, in order to efficiently identify them other models would be better suited (the use of texture analysis methods should be considered as well). Some of these nodules were missed because their pixel value distribution varied considerably from the template's. Some suspect regions were detected in areas outside the lungs but those were simply the results of the simple implemented segmentation; it

could be avoided by use of a more advanced search area selection.

We believe that the main error source for the project occurs at the suspicious regions binarization phase, because frequently their histogram shapes aren't bimodal, the two lobes not beeing clearly separated; there are cases were there is no gap between the peaks of each lobe and others were there is only a single lobe: all these factors degenerate in a serious malfunction of the used threshold selection method.
These are situations where for example:
- the circular structure is superimposed on the border of a rib or located in the pulmonary apex (they have approx. the same intensity values and therefore the biggest peak occurs for the right lobe: the threshold is selected to high);
- the subregion contrast is very bad (there is little difference between the nodule and background intensities: there is a single lobe);
- the nodule is attached to a vessel (the same situation as in rib overlaping).
The morphological operations applied to the first binarized set can also be destructive in the cases which the biggest connected component area is originally small.
We believe that is extremely difficult to detect nodules attached to vessels near the bronchus because it is hard to dintinguish between the two.

To finalize, we think that our low performance is caused by the simplicity of the used template besides the more important binarization problem, but it was possible to detect typical circular strutures correctly, so, this implies that our method is useful in principle. So if we can improve the binary thresholding quality we believe that much better results will be obtained using the same classification features and even the same model.

REFERENCES

[1] Gonzalez, Rafael C., *Digital image processing*, Prentice Hall, 2002

[2] Pratt, William K, *Digital image processing*, John Wiley & Sons, 1991

[3] M. Monteiro, A. Mendonça, A. Campilho, "Lung Field Detection on Chest Radiographs", INEB, Portugal, 2002

[4] Y. Lee, T. Hara, and H. Fujita, "Automated Detection of Pulmonary Nodules in Helical CT Images Based on an Improved Template-Matching Technique", IEEE Trans. Med. Imag, Vol. 20, No. 7, 2001

[5] A. Jain, *Fundamentals of Digital Image Processing*, Prentice Hall, 1989

[6] L. Alexandre, M. Silva, A. Campilho, "Detection of the costal diaphragmatic angle in chest radiographs"

[7] B. van Ginneken, Bart M. ter Haar Romeny, M. A. Viergever, "Computer-Aided Diagnosis in Chest Radiography:A Survey", IEEE Trans. Med. Imag, Vol. 20, No. 12, 2001

[8] M. Penedo, M. Carreira, A. Mosquera, D. Cabello, "Computer-Aided Diagnosis: A Neural-Network Based Approach to Lung Nodule Detection", IEEE Trans. Med. Imag, Vol. 17, No. 6, 1998

[9] M. Wirth, Lecture notes for Image Processing Algorithms and Applications, University of Guelph, 2003

[10] M. Sonka, J. Fitzpatrick, *Handbook of Medical Imaging*, SPIE Press